Supplementary Information

Supplementary Figure 1

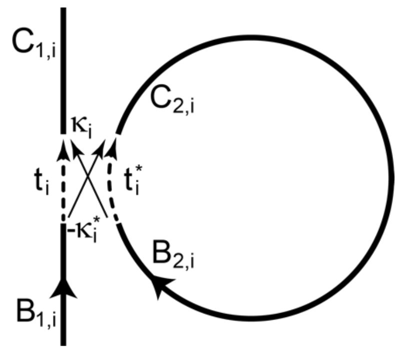

Supplementary Figure 1 Diagram of coupling between a ring resonator and a waveguide. t_i and κ_i are the through- and cross-coupling coefficients, respectively. i represents f or SH. $B_{n,i}$ and $C_{n,i}$ are the mode amplitudes.

Supplementary Table

Supplementary Table 1. Microdisk quality factors and associated loss and transmission coefficients at fundamental and SH wavelengths.

	Q_i^0	Q_i^{tot}	Q_i^c	$1-\alpha_i$	$1-\lvert t_i \rvert$
Fundamental	33000	16000	31000	2.2×10^{-3}	2.4×10^{-3}
SH	9000	4000	7200	2.9×10^{-2}	3.6×10^{-2}

Supplementary Discussion

Equation (1) in the main text,

$$\frac{dA_{\mathrm{SH}}}{d\theta} = A_{\mathrm{f}}^{2}\left(K_{+}e^{i(\Delta m+2)\theta} + K_{-}e^{i(\Delta m-2)\theta}\right), \quad \text{(S1)}$$

describes second-harmonic generation (SHG) in a cylindrically symmetric, nonlinear-optical microdisk made of a material from the $\bar{4}3\mathrm{m}$ crystal class. The equation is derived[11] by considering the projection of the $\chi^{(2)}$ nonlinear susceptibility tensor for these crystals in the cylindrical propagation geometry, which we summarize here. The nonlinear interaction is governed by the wave equation with a nonlinear-optical driving polarization, $\mathbf{P}^{NL}$

$$\nabla^2\mathbf{E} - \mu\varepsilon\frac{\partial^2\mathbf{E}}{\partial t^2} = \mu_0\frac{\partial^2\mathbf{P}^{NL}}{\partial t^2}. \quad \text{(S2)}$$

Consider the $\hat{z}$-component of the second-harmonic (SH) field. In cylindrical coordinates utilizing the slowing varying envelope approximation, Eq. (S2) can be approximated as

$$2im_{\mathrm{SH}}\frac{\partial E_{\mathrm{SH},z}}{\partial\theta} = \mu_0\omega_{\mathrm{SH}}^{2}P_{\mathrm{SH},z}^{NL}\exp(-i\Delta m\theta) \quad \text{(S3)}$$

where $\Delta m = m_{\mathrm{SH}} - 2m_{\mathrm{f}}$. In GaAs and other $\bar{4}3\mathrm{m}$ point-group symmetry crystals, there is only one non-zero $\chi^{(2)}$ tensor element: $d_{xyz} = d_{14} = d_{25} = d_{36}$, so that

$$P_{\mathrm{SH},z}^{\mathrm{NL}} = 2\varepsilon_0 d_{14}E_{\mathrm{f},x}E_{\mathrm{f},y}. \quad \text{(S4)}$$

In terms of $E_{\mathrm{f},r}$ and $E_{\mathrm{f},\theta}$,

$$\begin{aligned} E_{\mathrm{f},x} &= E_{\mathrm{f},r}\cos\theta - E_{\mathrm{f},\theta}\sin\theta \\ E_{\mathrm{f},y} &= E_{\mathrm{f},r}\sin\theta + E_{\mathrm{f},\theta}\cos\theta \\ P_{\mathrm{SH},z}^{\mathrm{NL}} &= 2\varepsilon_0 d_{14}\left\{E_{\mathrm{f},r}E_{\mathrm{f},\theta}\cos2\theta + \frac{1}{2}(E_{\mathrm{f},r}^{2} - E_{\mathrm{f},\theta}^{2})\sin2\theta\right\} \end{aligned}. \quad \text{(S5)}$$

Combining Eqs. (S3) through (S5), we obtain

$$\frac{\partial E_{\mathrm{SH},z}}{\partial\theta}=\frac{-i\mu_0\varepsilon_0 d_{14}\omega_{\mathrm{SH}}{}^2}{m_{\mathrm{SH}}}\left\{e^{-i(\Delta m-2)}\left[E_{\mathrm{f},r}E_{\mathrm{f},\theta}-\frac{i}{2}\left(E_{\mathrm{f},r}{}^2-E_{\mathrm{f},\theta}{}^2\right)\right]\right.$$
$$\left.+e^{-i(\Delta m+2)}\left[E_{\mathrm{f},r}E_{\mathrm{f},\theta}+\frac{i}{2}\left(E_{\mathrm{f},r}{}^2-E_{\mathrm{f},\theta}{}^2\right)\right]\right\}. \quad \text{(S6)}$$

The cylindrical propagation geometry together with the crystal symmetry produce quasi-phasematched frequency conversion when Δm = +2 or -2.

To calculate the nonlinear coupling coefficients, K_+ and K_- in Eq. (S1), a more careful analysis is needed. For a general three-frequency $\chi^{(2)}$ process inside a $\hat{z}$-surface-normal microdisk, the d_{xyz} tensor element requires one TM-polarized wave to interact with two TE-polarized waves; for SHG, the fundamental wave is TE-polarized $(H_{\mathrm{f},z},E_{\mathrm{f},r},E_{\mathrm{f},\theta})$ while the SH wave is TM-polarized $(E_{\mathrm{SH},z},H_{\mathrm{SH},r},H_{\mathrm{SH},\theta})$. $H_{\mathrm{f},z}$ and $E_{\mathrm{SH},z}$ are separable functions that can be written as

$$F_{i,z}(r,\theta,z)\exp(i\omega_i t)=A_i(\theta)\tilde{\psi}_i(r)\tilde{Z}_i(z)\exp[i(\omega_i t-m_i\theta)]\ , \quad \text{(S7)}$$

where $F_{i,z}=H_{\mathrm{f},z}$ or $E_{\mathrm{SH},z}$, and the normalization is chosen such that $\left|A_i(\theta)\right|^2$ represents the circulating power. The $\hat{r}$ and $\hat{\theta}$ components of the waves may be calculated from the $\hat{z}$ components by

$$\begin{array}{ll}
\mathrm{TM}=\{E_z,H_r,H_\theta\} & \mathrm{TE}=\{H_z,E_r,E_\theta\} \\
H_r=\dfrac{m}{r\mu_0\omega}E_z & E_r=-\dfrac{m}{r\varepsilon_0 n^2\omega}H_z \\
H_\theta=\dfrac{1}{i\mu_0\omega}\dfrac{\partial E_z}{\partial r} & E_\theta=\dfrac{i}{\varepsilon_0 n^2\omega}\dfrac{\partial H_z}{\partial r}
\end{array}\ , \quad \text{(S8)}$$

where μ_0 and ε_0 are the vacuum permeability and permittivity, respectively; c is the speed of light and n is the refractive index.

Considering the $\hat{z}$ component of the wave equation (Eq. (S2)), one can expand $E_{\mathrm{SH},z}$ in terms of the eigenmodes of the microdisk. If we focus on one particular SH resonance characterized by integers (m_{SH}, p_{SH}, q_{SH}) that are the azimuthal, radial and vertical indices, respectively, then the nonlinear coupling is calculated from the overlap integral between this SH eigenmode and $P_{\mathrm{SH},z}^{\mathrm{NL}}$, which is a function of the fundamental wave that we assume is also on-resonance. For a SH eigenmode characterized by $E_{\mathrm{SH},z} = A_{m_{\mathrm{SH}}p_{\mathrm{SH}}q_{\mathrm{SH}}}(\theta)\tilde{\psi}_{p_{\mathrm{SH}}}(r)\tilde{Z}_{q_{\mathrm{SH}}}(z)\exp[-im_{SH}\theta]$ and a fundamental eigenmode characterized by $H_{\mathrm{f},z} = A_{m_{\mathrm{f}}p_{\mathrm{f}}q_{\mathrm{f}}}(\theta)\tilde{\psi}_{p_{\mathrm{f}}}(r)\tilde{Z}_{q_{\mathrm{f}}}(z)\exp[-im_f\theta]$, the result of using $P_{\mathrm{SH},z}^{\mathrm{NL}}$ in Eq. (S5) with $E_{\mathrm{f},r}$ and $E_{\mathrm{f},r\theta}$ calculated from Eq. (S8), applying the slowly varying envelope approximation, and performing the overlap integral is[11]

$$\begin{aligned}\frac{\partial A_{m_{\mathrm{SH}}p_{\mathrm{SH}}q_{\mathrm{SH}}}}{\partial\theta} = \frac{-d_{14}}{2\varepsilon_0\omega_{\mathrm{SH}}}\left(\frac{A_{m_{\mathrm{f}}p_{\mathrm{f}}q_{\mathrm{f}}}}{n_{\mathrm{f}}^2}\right)^2 \int_{-h/2}^{h/2}\tilde{Z}_{q_{\mathrm{SH}}}(z)\tilde{Z}_{q_{\mathrm{f}}}^2(z)dz \times \\ \left[\begin{array}{l}\int_0^R e^{i(\Delta m+2)\theta} r\tilde{\psi}_{\mathrm{SH}}\left(\frac{m_f}{r}\tilde{\psi}_f + \frac{\partial\tilde{\psi}_f}{\partial r}\right)^2 dr \\ \qquad -\int_0^R e^{i(\Delta m-2)\theta} r\tilde{\psi}_{\mathrm{SH}}\left(\frac{m_f}{r}\tilde{\psi}_f - \frac{\partial\tilde{\psi}_f}{\partial r}\right)^2 dr\end{array}\right],\end{aligned} \tag{S9}$$

where R and h are the radius and height of the microdisk, respectively. Comparing Eq. (S9) to Eq. (S1), we identify

$$\begin{aligned}K_+ &= -\frac{d_{14}}{2\varepsilon_0\omega_{SH}n_{\mathrm{f}}^4}\int_{-h/2}^{h/2}\tilde{Z}_{q_{\mathrm{SH}}}(z)\tilde{Z}_{q_{\mathrm{f}}}^2(z)dz\int_0^R r\tilde{\psi}_{\mathrm{SH}}\left(\frac{m_{\mathrm{f}}}{r}\tilde{\psi}_{\mathrm{f}} + \frac{\partial\tilde{\psi}_{\mathrm{f}}}{\partial r}\right)^2 dr \\ K_- &= \frac{d_{14}}{2\varepsilon_0\omega_{\mathrm{SH}}n_{\mathrm{f}}^4}\int_{-h/2}^{h/2}\tilde{Z}_{q_{\mathrm{SH}}}(z)\tilde{Z}_{q_{\mathrm{f}}}^2(z)dz\int_0^R r\tilde{\psi}_{\mathrm{SH}}\left(\frac{m_{\mathrm{f}}}{r}\tilde{\psi}_{\mathrm{f}} - \frac{\partial\tilde{\psi}_{\mathrm{f}}}{\partial r}\right)^2 dr\ .\end{aligned} \tag{S10}$$

For second-harmonic generation in a 2.6-μm radius and 160-nm thickness GaAs microdisk between a TE-polarized fundamental (m_f=13, p_f=1, q_f=1) and TM-polarized second harmonic (m_{SH}=24, p_{SH}=2, q_{SH}=1), we calculate $K_+ = 1.6\times10^{-3}$ $W^{-1/2}$ and $K_- = -1.0\times10^{-5}$ $W^{-1/2}$, where λ_f = 1.99 μm, n_f = 3.34, and d_{14} = 94 pm/V [27].

The coupling of a waveguide to a ring resonator can be described by the sketch in Fig. S1. $B_{n,i}$ and $C_{n,i}$ are the complex mode amplitudes normalized such that $|B_{n,i}|^2$, $|C_{n,i}|^2$ = power. In the absence of reflections, coupling between the resonator and waveguide is described by[36]

$$\begin{bmatrix} C_{1,i} \\ C_{2,i} \end{bmatrix} = \begin{bmatrix} t_i & \kappa_i \\ -\kappa_i^* & t_i^* \end{bmatrix} \begin{bmatrix} B_{1,i} \\ B_{2,i} \end{bmatrix}. \tag{S11}$$

The coupler is taken to be lossless so that $|\kappa_i|^2 + |t_i|^2 = 1$. At the fundamental wave,

$$B_{2,\mathrm{f}} = \alpha_{\mathrm{f}} \exp(i\varphi_{\mathrm{f}}) C_{2,\mathrm{f}}, \tag{S12}$$

where α_f is the resonator loss, and ϕ_f is the phase accumulated by propagation around the resonator. At the SH wave, there is loss (α_{SH}), phase shift (ϕ_{SH}) and SHG gain. By integrating Eq. (S1) from $\theta = 0$ to 2π, we find that each round trip in the microdisk produces an increase in the SH amplitude

$$\begin{aligned} A_{\mathrm{SH}}(2\pi) - A_{\mathrm{SH}}(0) &= 2\pi A_{\mathrm{f}}^2 \left(K_+ e^{i(\Delta m+2)\pi} \mathrm{sinc}[(\Delta m + 2)\pi] + K_- e^{i(\Delta m-2)\pi} \mathrm{sinc}[(\Delta m - 2)\pi] \right) \\ &= A_{\mathrm{f}}^2 \tilde{K} \end{aligned} \tag{S13}$$

where sinc(x) = sin(x)/x and $A_{\mathrm{f}} \approx$ constant. Combining Eq. (S13) with phase shift and loss, we obtain

$$\frac{B_{2,\mathrm{SH}}}{\alpha_{\mathrm{SH}} \exp(i\varphi_{\mathrm{SH}})} - C_{2,\mathrm{SH}} = \left| C_{2,\mathrm{f}} \right|^2 \tilde{K} \ . \tag{S14}$$

Equations (S11) and (S12) imply that the circulating power is

$$\left| B_{2,\mathrm{f}} \right|^2 = \frac{\alpha_{\mathrm{f}}^2 \left(1 - |t_{\mathrm{f}}|^2 \right)}{1 + \alpha_{\mathrm{f}}^2 |t_{\mathrm{f}}|^2 - 2\alpha_{\mathrm{f}} |t_{\mathrm{f}}| \cos(\psi_{\mathrm{f}} + \varphi_{\mathrm{f}})} \left| B_{1,\mathrm{f}} \right|^2 \ , \tag{S15}$$

where $t_i = |t_i| \exp(-i\psi_i)$. Note that Eq. (S15) also describes the circulating-power spectrum of a “passive” resonator in the SH wavelength range.

Combining Eqs. (S11) and (S14) with $B_{1,SH} = 0$, we find

$$\begin{aligned}\left|C_{1,\mathrm{SH}}\right|^2 &= \left(1-|t_{\mathrm{SH}}|^2\right)\left|B_{2,\mathrm{SH}}\right|^2 \\ &= \left|B_{2,\mathrm{f}}\right|^4 \frac{\left(1-|t_{\mathrm{SH}}|^2\right)\left|\tilde{K}\right|^2 \alpha_{\mathrm{SH}}{}^2}{1+\alpha_{\mathrm{SH}}{}^2|t_{\mathrm{SH}}|^2-2\alpha_{\mathrm{SH}}|t_{\mathrm{SH}}|\cos(\psi_{\mathrm{SH}}+\varphi_{\mathrm{SH}})} \\ &= \left|B_{1,\mathrm{f}}\right|^4 \frac{\left(1-|t_{\mathrm{SH}}|^2\right)\left|\tilde{K}\right|^2 \alpha_{\mathrm{SH}}{}^2}{1+\alpha_{\mathrm{SH}}{}^2|t_{\mathrm{SH}}|^2-2\alpha_{\mathrm{SH}}|t_{\mathrm{SH}}|\cos(\psi_{\mathrm{SH}}+\varphi_{\mathrm{SH}})} \\ &\qquad \times\left(\frac{\alpha_f{}^2(1-|t_{\mathrm{f}}|^2)}{1+\alpha_{\mathrm{f}}{}^2|t_{\mathrm{f}}|^2-2\alpha_{\mathrm{f}}|t_{\mathrm{f}}|\cos(\psi_{\mathrm{f}}+\varphi_{\mathrm{f}})}\right)^2 .\end{aligned} \tag{S16}$$

$\left|B_{2,\mathrm{f}}\right|^2$ and $\left|B_{2,\mathrm{SH}}\right|^2$ are the circulating powers at the fundamental and SH, respectively, while $\left|C_{1,\mathrm{f}}\right|^2$ and $\left|C_{1,\mathrm{SH}}\right|^2$ are the output powers. Comparison of Eqs. (S16) to (S15) yields Eq. (3) in the main text.

The phase shifts (φ_{f} and φ_{SH}) are related to the azimuthal numbers m_i of the resonances. m_i plays a role analogous to the wavevector k_i in linear propagation geometries; both describe the rate of phase accumulation due to propagation. Even though m_i is only well-defined at resonant wavelengths, we can estimate an effective $m_i'(\lambda_i)$ for all wavelengths inside the microdisk by interpolating between resonances of the same spatial-mode family. The continuous function $m_i'(\lambda_i)$ allows us to calculate ϕ_i for all wavelengths, both on- and off-resonance with the cavity. The phase mismatch accumulated per round trip is then

$$-2\pi\Delta m' = \varphi_{\mathrm{SH}} - 2\varphi_{\mathrm{f}} \;, \tag{S17}$$

so $\tilde{K}$ defined in Eq. (S12) is a function of φ_{f} and φ_{SH}. The loss, α_i, and transmission coefficient, $|t_i|$, can be calculated from the intrinsic Q_i^0 and coupling Q_i^c quality factors by[11,36]

$$Q_i^0 = \pi\frac{\sqrt{\alpha_i}}{1-\alpha_i}\frac{c}{\lambda_i\,\delta f_{i,FSR}} \qquad\qquad Q_i^c = \pi\frac{\sqrt{|t_i|}}{1-|t_i|}\frac{c}{\lambda_i\,\delta f_{i,FSR}} \,, \tag{S18}$$

where $\delta f_{i,FSR}$ is the free spectral range of the resonator for wave *i* in frequency units.

For the resonant modes of the GaAs microdisk considered here, $\delta f_{f,FSR} = 6.4\times10^{12}$ Hz and $\delta f_{SH,FSR} = 3.6\times10^{12}$ Hz. The measured quality factors are summarized in Table S1, as are the calculated loss and transmission coefficients (Eq. (S18)) at both wavelengths. Using finite-element modeling, we calculate the wavelengths for several adjacent resonances near the fundamental (m_f=13, p_f=1, q_f=1) and second harmonic (m_{SH}=24, p_{SH}=2, q_{SH}=1) resonances in order to construct $m_i'(\lambda_i)$. We then used Eq. (S16) and $\phi_i = -2\pi m_i'(\lambda_i)$ to calculated the round-trip phases. Using values for the loss and transmission coefficients in Table S1, $K_+ = 1.6\times10^{-3}$ $W^{-1/2}$ and $K_- = -1.0\times10^{-5}$ $W^{-1/2}$ calculated earlier, and taking $\psi_f = \psi_{SH} = 0$, Eq. (S16) predicts peak, normalized conversion efficiency $\eta = |C_{1,SH}|^2/|B_{1,f}|^4 = 1\times10^{-3}$/mW for a microdisk with || $|\lambda_f^{res} - 2\lambda_{SH}^{res}| = 2.2$ nm. By decreasing the theoretical microdisk radius by 9 nm, $|\lambda_f^{res} - 2\lambda_{SH}^{res}| = 0$ nm and the theoretical peak, normalized conversion efficiency increases to $\eta = 8\times10^{-2}$/mW. We note that the GaAs microdisk described here may also supports $\bar{4}$-QPM between the fundamental (m_f=13, p_f=1, q_f=1) resonance and the second harmonic (m_{SH}=28, p_{SH}=1, q_{SH}=1) resonance (Δm = +2). As calculated in Ref. 11, the nonlinear coupling coefficients for these modes are $K_+ = 9.7\times10^{-4}$ $W^{-1/2}$ and $K_- = -1.9\times10^{-3}$ $W^{-1/2}$. If $|\lambda_f^{res} - 2\lambda_{SH}^{res}| = 0$ nm for the resonances satisfying Δm = +2, then the normalized conversion efficiency would be $\eta = 1.2\times10^{-1}$/mW.

Supplementary Reference

34. Yariv, A. Universal relations for coupling of optical power between microresonators and dielectric waveguides. *Electron. Lett*. **36**, 321–322 (2000).